IOP Publishing Journal of Optics
J. Opt. 19 (2017) 124017 (6pp) https://doi.org/10.1088/2040-8986/aa9865

Single-shot carrier-envelope-phase tagging using an *f*–2*f* interferometer and a phase meter: a comparison

Xiaoming Ren[1,2], A M Summers[1], Kanaka Raju P[1], Aram Vajdi[1], Varun Makhija[1,3], C W Fehrenbach[1], Nora G Kling[1,4], K J Betsch[1], Z Wang[1], M F Kling[1,5,6], K D Carnes[1], I Ben-Itzhak[1], Carlos Trallero-Herrero[1,4,7] and Vinod Kumarappan[1,7]

[1] J.R. Macdonald Laboratory, Physics Department, Kansas-State University, 116 Cardwell Hall, Manhattan, KS 66506, United States of America
[2] Institute for the Frontier of Attosecond Science and Technology, CREOL, Department of Physics, University of Central Florida, Orlando, FL 32816, United States of America
[3] Department of Physics, University of Ottawa, 150 Louis Pasteur, Ottawa, ON K1N 6N5, Canada
[4] Department of Physics, University of Connecticut, Storrs, CT 06269, United States of America
[5] Max Planck Institute of Quantum Optics, D-85748 Garching, Germany
[6] Department of Physics, Ludwig-Maximilians-Universität Munich, D-85748 Garching, Germany

E-mail: carlos.trallero@uconn.edu and vk@phys.ksu.edu

Received 30 June 2017, revised 10 October 2017
Accepted for publication 25 October 2017
Published 29 November 2017

Abstract

Carrier-envelope phases (CEPs) from a kHz repetition rate, non-CEP stabilized laser system are measured and tagged with two different methods: an *f*–2*f* interferometer and a stereo-above-threshold-ionization carrier-envelope-phase-meter. Both methods utilize the octave spanning spectrum generated in the hollow-core fiber (HCF) that broadens the laser spectrum to produce few-cycle pulses. Phases from both methods are carefully synchronized and compared on a single shot level. The results show that the CEPs measured by both methods are in good agreement and demonstrate that a HCF based *f*–2*f* interferometer is well suited for CEP tagged experiments.

Keywords: carrier envelope phase tagging, few-cycle pulses, ultrafast science

(Some figures may appear in colour only in the online journal)

1. Introduction

As ultrafast science moves towards shorter and shorter time scales, laser sources with pulse durations in the few to sub-femtosecond regime become more desirable [1]. For Ti:sapphire lasers, which are commonly used nowadays, the bandwidth of the laser pulses can be broadened by self-phase-modulation through propagation in a hollow-core fiber (HCF) filled with a noble gas [2]. By properly compensating for the dispersion with chirped mirrors, pulse durations as short as 3 fs can be achieved [3]. For a center wavelength of ~800 nm, this is close to one optical cycle. In this regime, the shape of the laser electric field plays an important role in strong-field processes [4]. Therefore, the control of the carrier-envelope phase (CEP)—the offset between the peak of the electric field and the peak of the envelope—is crucial. Propelled by the need for precision in laser frequency metrology [5], methods for the stabilization of the CEP developed rapidly for Ti:sapphire oscillators [6] and amplifiers [7, 8]. This has enabled numerous seminal efforts such as single isolated attosecond pulse generation [9] and multi-octave waveform synthesis [10, 11]. Nowadays, oscillator technology and stability have evolved to the point where it is possible to lock the CEP for long periods of time utilizing *f*–2*f* [6] interferometry. However, for amplifier systems, especially with high pulse energies, the large scale of the systems and CEP jitter through grating-based stretchers and compressors [12, 13] introduces a significant amount of CEP noise.

[7] Authors to whom any correspondence should be addressed.

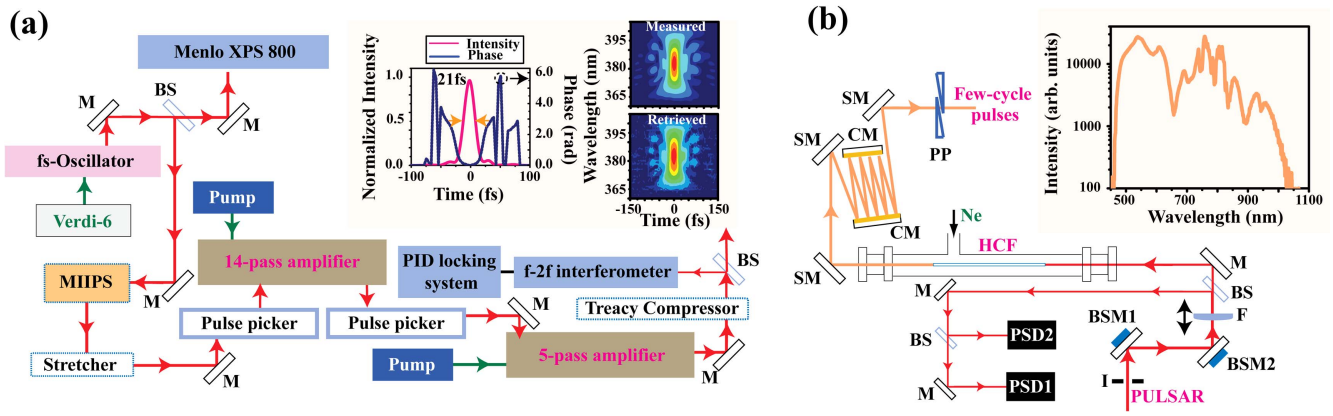

Figure 1. (a) Schematic of the PULSAR laser system. M: mirror; BS: beam splitter; MIIPS: multiphoton intrapulse interference phase scan; PID locking system: proportional, integral, derivative locking system. Inset shows results from a typical SHG-FROG pulse measurement. (b) High repetition rate few-cycle pulse generation system. I: Iris; BSM: beam stabilization mirror; F: lens; BS: beam splitter; M: mirror; PSD: position sensitive detector; HCF: hollow-core fiber; SM: low-dispersive broadband silver mirror; CM: chirped mirror; PP: prism pair. Inset shows octave-spanning spectrum generated through this process.

Although it is possible to lock the CEP to within 140 mrad (root mean square error) for short time periods (minutes) [14] or 300 mrad for longer time periods (hours) [15] using a feedback signal from an *f*–2*f* interferometer, a stereo above-threshold-ionization carrier-envelope phase meter (CEPM) [16], or feed forward methods [14, 17, 18], it is still quite challenging to maintain a good CEP lock for the amplified pulses for very long periods of time.

An alternate way of studying CEP-dependent processes is to record the CEP value for each pulse. This measurement can then be synchronized with the observable data. This technique is known as CEP tagging [19] and does not require the laser pulses to be CEP locked. However, several other conditions need to be satisfied. First, CEP values need to be measured on a single-shot basis. Additionally, the acquisition rate of the single-shot CEP should ideally be at the level of the laser repetition rate (now typically several kHz) to allow enough statistics for reconstructing the CEP dependence. These conditions are readily satisfied by the CEPM [19]. As such, the CEPM has emerged as a standard method for CEP tagging experiments [20–26]. Single-shot CEP measurements for mJ amplified systems have also been performed using an *f*–2*f* interferometer in the past [21, 27–30]. Here, we show, to the best of our knowledge, the first single-shot, direct comparison of a CEPM and an *f*–2*f* interferometer. Our results demonstrate that *f*–2*f* interferometry is an accurate and robust way to tag CEP values. In the following experiment, the PULSAR laser is running without CEP locking, which is the typical operational mode in CEP tagged experiments.

2. Generation of intense few-cycle pulses at high repetition rates

In this study, we use a Ti:sapphire chirped-pulse-amplification laser system (KM Labs, customized Red Dragon) for the production of intense, few-cycle pulses, at a repetition rate of 10 kHz. The laser, shown schematically in figure 1(a), which we refer to as PULSAR, produces 10 kHz of CEP-locked, 2 mJ, 21 fs pulses. In the first stage, a multiphoton intrapulse interference phase scan system (Biophotonic Solutions) is used to apply a tunable spectral-phase profile to the seed pulses [31] and is manually adjusted to precisely compensate for higher-order dispersion throughout. This high-order compensation allows for the short pulse duration at the output of the amplifier. The inset in figure 1(a) shows the measured second-harmonic generation frequency-resolved-optical gating (SHG-FROG) spectrogram as well as the retrieved electric field phase and amplitude. The SHG-FROGs were done using a commercial device (Mesa Photonics) and have an error of 0.3%. The laser is similar in design and CEP control to the one described in [15]. Some of the main differences between both lasers are in the repetition rate, pulse duration and the CEP RMS noise (∼400 mrad). However, PULSAR is normally operated in free running mode (no CEP locking), with shot-to-shot CEP tagging. Single-shot tagging is better suited for our long (on the order of several days) coincidence momentum imaging measurements [20] versus trying to control the CEP over such long periods of time.

In order to produce few-cycle pulses [32], we couple ∼0.9 mJ, 21 fs pulses from the PULSAR laser system into an inert-gas-filled HCF as shown in figure 1(b). A 1.5 m focal length plano-convex lens is used to focus the laser beam into a 1 m long HCF with 250 μm inner diameter filled with ∼2.4 bar of Ne gas. The HCF system generates an octave-spanning spectrum from 500 to 1000 nm through self-phase modulation (figure 1(b) inset). A small portion of the PULSAR beam, split off before the HCF, is used for beam pointing stabilization. The output of the HCF goes through a set of ultra-broadband chirped mirrors (UltraFast Innovations, PC70; $-50\,\mathrm{fs}^2$ per reflection at 800 nm) to compensate the positive dispersion due to propagation through the fiber. A pair of fused-silica wedges (LENS-Optics) is used to control the small residual dispersion. Ultimately, this allows for the generation of 5 fs pulses with 0.4 mJ of energy at 10 kHz repetition rate. The pulse duration was estimated from radius of the parametric asymmetry plot (PAP), as described in [33],

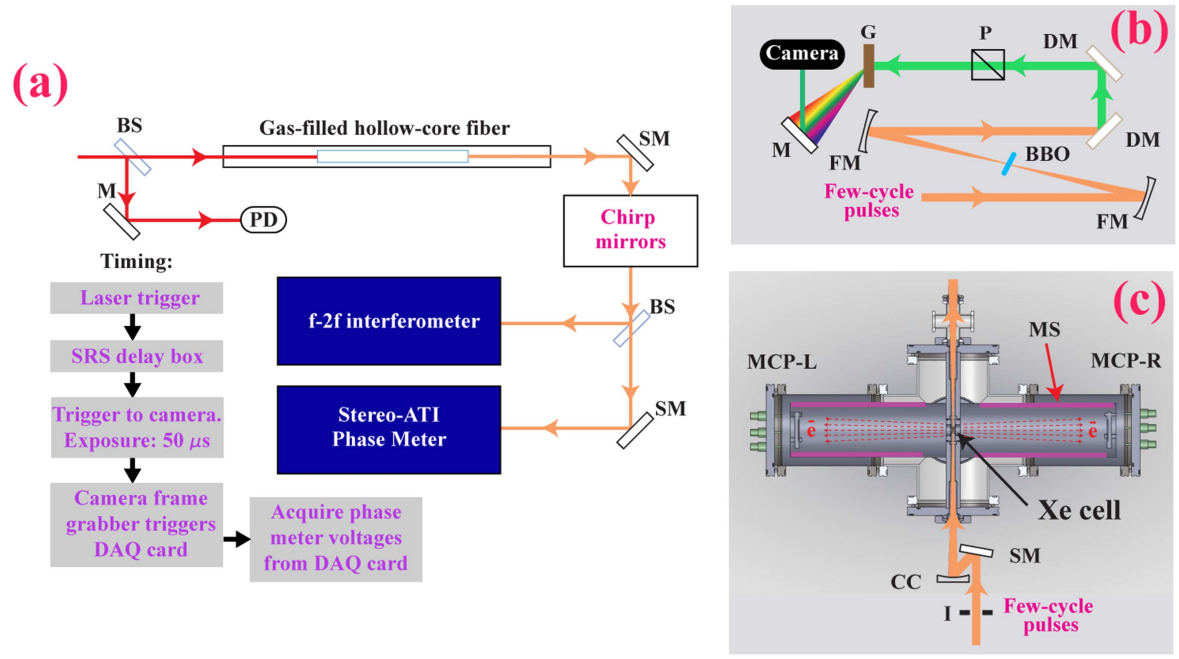

Figure 2. (a) Experimental setup. BS: beam spliter; M: pointing stabilizing mirror; PD: photodiode (b) *f*–2*f* interferometer. FM: focusing mirror; DM: dichroic mirror; P: polarizer; G: grating (c) CEPM (described in detail in [34]). I: iris; SM: silver mirror; CC: concave mirror; MS: μ-metal shield; MCP: micro channel plate; Xe cell: xenon gas cell.

as well as from results in previous studies using the same setup [25].

3. High-repetition rate carrier envelope phase tagging

The shot-to-shot carrier envelope phase of the system is monitored using the CEPM [19], as shown in figure 2(c). To use the CEPM, a portion of the few-cycle-pulse beam (typically $\sim$40 μJ) is focused using an $f = 25$ cm spherical mirror onto the phase meter. The 5 fs pulses ionize the target gas at the focus located inside a gas cell filled with Xe at $\sim 1.3 \times 10^{-6}$ bar. The generated direct (low energy) and backscattered (high energy) electrons are detected using two microchannel plate detectors (Photonis, APD 2 MA25/12/10/12 D 60:1) on both sides of the phase meter (MCP-L & MCP-R). The signals from each of the detectors are processed by dedicated electronics[8] which integrate the signals on the left and right detectors within the low and high energy regions ($\mathrm{TOF_{low}}$ and $\mathrm{TOF_{high}}$) respectively. From this, the normalized difference, $A_{\mathrm{low,high}} = (N_L - N_R)/(N_L + N_R)$ is calculated. During data acquisition, both values are output from the phase meter and recorded as positive voltages. Plotting A_{low} versus A_{high} results in a PAP, shown figure 3(c). This provides the carrier envelope phase information shot by shot [19, 23, 34]. From the PAP, a one-to-one mapping of the polar angle of each individual hit and the single-shot CEP value can be established.

[8] The original electronics used in this system were developed at MPQ/LMU. The system was recently upgraded to new electronics from IOQ, JENA [23].

With the overall goal of comparing the CEPM to an all optical *f*–2*f* CEP measurement, an additional small portion of the few-cycle pulse is also picked off and sent to the *f*–2*f* interferometer, depicted in figure 2(b). In this interferometer, a beta-barium-borate crystal doubles the frequency of the red end ($\sim$1000 nm) of the octave-spanning spectrum produced in the HCF. This doubled frequency then interferes with the blue end ($\sim$500 nm) of the original spectrum and produces an interference pattern in the spectral domain after a transmission grating. This *f*–2*f* interferometer differs from other common *f*–2*f* interferometers in that it does not include an inherent broadening stage. For non-octave-spanning pulses, it is necessary to first broaden the pulse, which is commonly done by white light generation in sapphire or a similar crystal. However, for our setup, this is unnecessary as the HCF already produces a broad enough pulse for *f*–2*f* self-referencing.

Figure 3(a) shows a spectrum for one laser shot and the line-out obtained by integrating in the vertical direction. This interference pattern can be mathematically expressed as $I(\omega) \propto I_{\mathrm{WL}}(\omega) + I_{\mathrm{SH}}(\omega) + 2\sqrt{I_{\mathrm{WL}}(\omega) I_{\mathrm{SH}}(\omega)} \cos(\omega\tau + \phi_{\mathrm{SH}}(\omega) - \phi_{\mathrm{WL}}(\omega) + \phi_{\mathrm{CE}})$, where $I_{\mathrm{WL}}(\omega)$ and $I_{\mathrm{SH}}(\omega)$ represent the intensities of the blue-end spectrum directly from the HCF output and frequency-doubled from the red end of the HCF output, respectively. τ is the delay between these two pulses, $\phi_{\mathrm{SH}}(\omega)$ and $\phi_{\mathrm{WL}}(\omega)$ denote the spectral phases of the frequency doubled portion and original portion out of the HCF, respectively, and ϕ_{CE} is the CEP. It is reasonable to assume that $\omega\tau + \phi_{\mathrm{SH}}(\omega) - \phi_{\mathrm{WL}}(\omega)$ stays constant for one particular frequency component, and thus the phase of $I(\omega)$ can be retrieved as the CEP plus a constant offset. We filtered the interference shown in figure 3(a) through a Hanning window to reduce high frequency noise and padded with

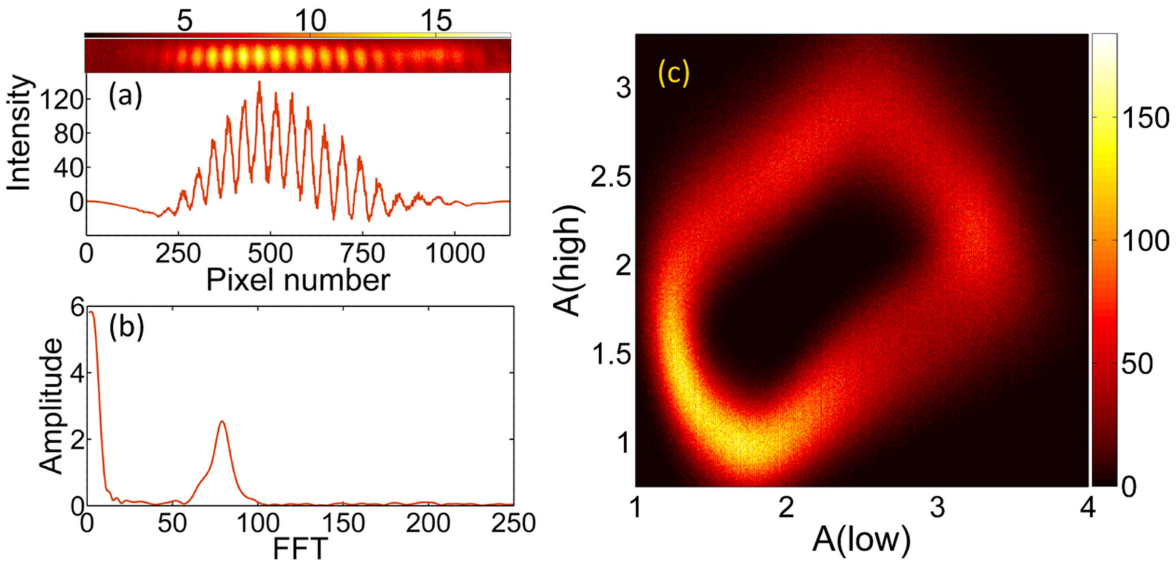

Figure 3. (a) Interference pattern for one laser shot. Fringes are obtained after integrating along the height of the image and applying a Hanning filter. (b) Amplitude of the FFT of the fringes. The relevant component is the peak shown around index 75 (c) Parametric asymmetry plot from the CEPM for 6 million laser shots where A(low) and A(high) are the respective low and high electron energy regions.

zeros to reduce low frequency noise. The spectrum is then Fourier transformed (FFT), and the relative CEP is extracted as the phase of the first, non-dc peak (at position around 75) in the time domain, shown in figure 3(b). It has been shown previously that a fast camera or spectrometer with sufficiently low exposure time is able to measure a single-shot interference pattern at high speed [12]. In our case, a Camera Link interface is able to transfer the images at kHz rates if the image size is small enough. Further, the FFT is carried out online and only the phase of each shot is saved at a CEP measurement rate of 600 Hz. A fast Basler A504k camera allows an acquisition rate of 1.8 kHz, and we anticipate a faster camera or linescan camera with Camera Link should allow for even faster acquisition if there is enough signal for each laser shot. It should be mentioned that other approaches, employing *f*–2*f* interferometry, produce acquisition rates at much faster speeds, by using diode arrays, photomultiplier tubes or avalanche photodiodes for spectral fringe acquisition. These methods can have much higher acquisition speeds but also suffer from other issues such as decreases in resolution [30, 35, 36].

4. Comparison of CEP tagging methods

In order to compare the single-shot CEP measured by the *f*–2*f* and the CEPM, the timing of the acquisition needs to be precisely controlled. A flow chart of the timing logic is shown in figure 2(a). The camera in the *f*–2*f* interferometer is triggered from a delayed photodiode signal and is exposed for a 50 μs window to allow for single-shot detection. At the same time, the frame grabber (NI PCIe-1433) sends a trigger to a National Instrument Data Acquisition (NI-DAQ) card inside the computer. The output signals from the CEPM processing electronics are then recorded by the DAQ card for the same laser shot that produced the *f*–2*f* interference pattern.

The results are shown in figure 4 panels (a) and (b). Specifically, panel (a) shows a shot-to-shot mapping of the CEP measured by the two methods for 6 million laser shots. Two narrow bands at 45 degrees are clearly observed, suggesting that the CEP measurements from the two are very well correlated with a constant phase difference of 0.9 rad. This constant phase offset depends on the beam path in each measurement arm. Figure 4 panel (b) shows the distribution of the shot-to-shot difference between the two measured CEP values. A standard deviation of 220 mrad is calculated from this difference. Möller *et al* [37] suggested that, for a 5 fs pulse, CEPM has a minimum CEP measurement uncertainty of about 120 mrad. Using this value, the uncertainty for the *f*–2*f* can then be estimated to be about 184 mrad. However, there is no guarantee that our CEPM has such a low uncertainty, suggesting that 184 mrad might be a high estimate for the CEP uncertainty for the *f*–2*f* interferometer. Overall, both of these uncertainties are of similar magnitude and leads us to the conclusion that both methods produce comparable accuracies for CEP tagging.

We have presented a method, based on *f*–2*f* interferometry, for single-shot CEP tagging with an estimated 184 mrad uncertainty and shown evidence that CEP-tagged experiments can be performed using an *f*–2*f* interferometer. This all-optical method is simpler and easier to operate than the CEPM. Additionally, it should be noted that as with the CEPM the *f*–2*f* interferometer requires few-cycle pulses to operate correctly. The CEPM has been shown to have an uncertainty in the single-shot phase value of ~350 mrad for an 8.5 fs pulse [37], and the *f*–2*f* interferometer presented requires an octave spanning pulse to operate. However, as almost all relevant studies examining CEP-dependent behavior also require few-cycle pluses, this should not be a

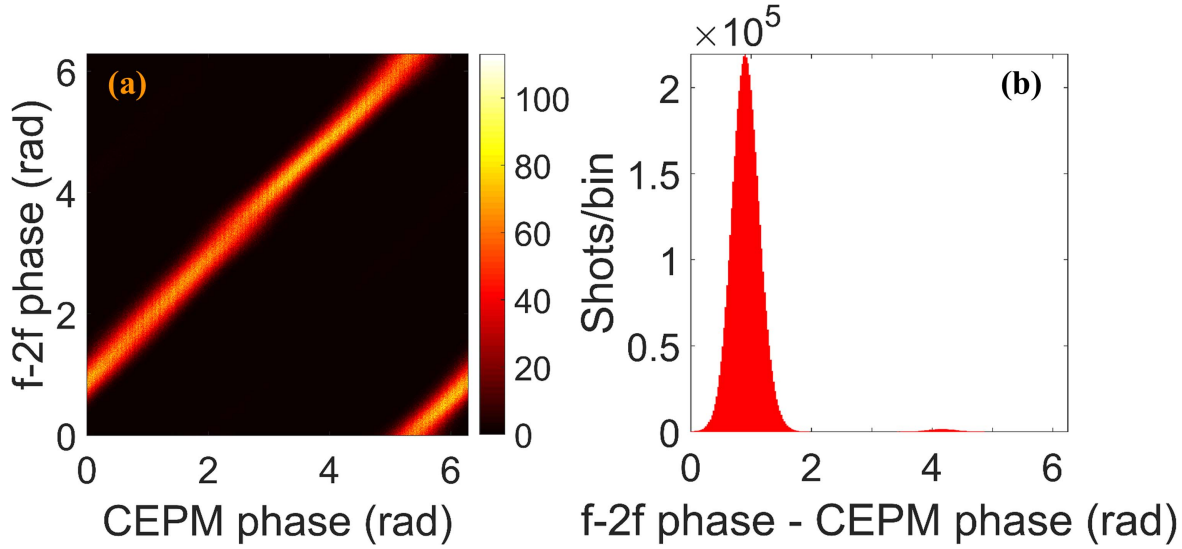

Figure 4. (a) Correlation of the single-shot CEP measured by the CEPM and HCF-based *f*–2*f* interferometer. (b) Histogram of the difference between the two phases; phases have been converted to within 0 to 2π.

significant limitation. We also note that the *f*–2*f* interferometer does not provide the absolute CEP while the CEPM in principle can [19]. However, since the CEP needs to be calibrated at the experiment in both cases, this is not a significant disadvantage.

Acknowledgments

The authors would like to thank Mohammad Zohrabi for assisting with the HCF and CEPM alignment as well as Ben Langdon and KM Labs for many useful discussions. This work is supported by the Chemical Sciences, Geosciences, and Biosciences Division, Office of Basic Energy Sciences, Office of Science, US Department of Energy under Grant No. DE-FG02-86ER13491. The laser was provided by Grant No. DE-FG02-09ER16115 from the same funding agency. X R acknowledges support by an NSF-MRI, grant No 1229674. AMS was supported by the Department of Defense (DoD) through the National Defense Science & Engineering Graduate Fellowship. MFK is grateful for support by the Max Planck Society and the DFG via the Munich Centre for Advanced Photonics.

ORCID iDs

A M Summers https://orcid.org/0000-0003-2694-4969
M F Kling https://orcid.org/0000-0002-1710-0775

References

[1] Krausz F and Ivanov M 2009 Attosecond physics *Rev. Mod. Phys.* **81** 163–234
[2] Nisoli M, De Silvestri S and Svelto O 1996 Generation of high energy 10 fs pulses by a new pulse compression technique *Appl. Phys. Lett.* **68** 2793–5
[3] Pervak V, Tikhonravov A V, Trubetskov M K, Naumov S, Krausz F and Apolonski A 2007 1.5-octave chirped mirror for pulse compression down to sub-3 fs *Appl. Phys.* B **87** 5–12
[4] Paulus G G, Grasbon F, Walther H, Villoresi P, Nisoli M, Stagira S, Priori E and Silvestri S De 2001 Absolute-phase phenomena in photoionization with few-cycle laser pulses *Nature* **414** 182–4
[5] Cundiff S T and Ye J 2003 Colloquium: femtosecond optical frequency combs *Rev. Mod. Phys.* **75** 325–42
[6] Jones D J, Diddams S A, Ranka J K, Stentz A, Windeler R S, Hall J L and Cundiff S T 2000 Carrier-envelope phase control of femtosecond mode-locked lasers and direct optical frequency synthesis *Science* **288** 635–9
[7] Baltuska A, Uiberacker M, Goulielmakis E, Kienberger R, Yakovlev V S, Udem T, Hansch T W and Krausz F 2003 Phase-controlled amplification of few-cycle laser pulses *IEEE J. Sel. Top. Quantum Electron.* **9** 972–89
[8] Kakehata M *et al* 2004 Carrier-envelope-phase stabilized chirped-pulse amplification system scalable to higher pulse energies *Opt. Express* **12** 2070–80
[9] Sansone G *et al* 2006 Isolated single-cycle attosecond pulses *Science* **314** 443–6
[10] Wirth A *et al* 2011 Synthesized light transients *Science* **334** 195–200
[11] Huang S-W *et al* 2011 High-energy pulse synthesis with sub-cycle waveform control for strong-field physics *Nat. Photon.* **5** 475–9
[12] Gagnon E, Thomann I, Paul A, Lytle A L, Backus S, Murnane M M, Kapteyn H C and Sandhu A S 2006 Long-term carrier-envelope phase stability from a grating-based, chirped pulse amplifier *Opt. Lett.* **31** 1866–8
[13] Chang Z 2006 Carrier-envelope phase shift caused by grating-based stretchers and compressors *Appl. Opt.* **45** 8350–3
[14] Lücking F, Crozatier V, Forget N, Assion A and Krausz F 2014 Approaching the limits of carrier-envelope phase stability in a millijoule-class amplifier *Opt. Lett.* **39** 3884–7
[15] Langdon B *et al* 2015 Carrier-envelope-phase stabilized terawatt class laser at 1 kHz with a wavelength tunable option *Opt. Express* **23** 4563–72
[16] Adolph D, Sayler A M, Rathje T, Rühle K and Paulus G G 2011 Improved carrier-envelope phase locking of intense few-cycle laser pulses using above-threshold ionization *Opt. Lett.* **36** 3639–41

[17] Koke S, Grebing C, Frei H, Anderson A, Assion A and Steinmeyer G 2010 Direct frequency comb synthesis with arbitrary offset and shot-noise-limited phase noise *Nat. Photon.* **4** 462–5
[18] Lücking F, Assion A, Apolonski A, Krausz F and Steinmeyer G 2012 Long-term carrier-envelope-phase-stable few-cycle pulses by use of the feed-forward method *Opt. Lett.* **37** 2076–8
[19] Wittmann T, Horvath B, Helml W, Schätzel M G, Gu X, Cavalieri A L, Paulus G G and Kienberger R 2009 Single-shot carrier-envelope phase measurement of few-cycle laser pulses *Nat. Phys.* **5** 357–62
[20] Johnson N G *et al* 2011 Single-shot carrier-envelope-phase-tagged ion-momentum imaging of nonsequential double ionization of argon in intense 4-fs laser fields *Phys. Rev.* A **83** 013412
[21] Sayler A M, Rathje T, Müller W, Rühle K, Kienberger R and Paulus G G 2011 Precise, real-time, every-single-shot, carrier-envelope phase measurement of ultrashort laser pulses *Opt. Lett.* **36** 1–3
[22] Süßmann F *et al* 2011 Single-shot velocity-map imaging of attosecond light-field control at kilohertz rate *Rev. Sci. Instrum.* **82** 093109
[23] Rathje T, Johnson N G, Möller M, Süßmann F, Adolph D, Kübel M, Kienberger R, Kling M F, Paulus G G and Sayler A M 2012 Review of attosecond resolved measurement and control via carrier-envelope phase tagging with above-threshold ionization *J. Phys. B: At. Mol. Opt. Phys.* **45** 074003
[24] Kübel M, Betsch K J, Johnson N G, Kleineberg U, Moshammer R, Ullrich J, Paulus G G, Kling M F and Bergues B 2012 Carrier-envelope-phase tagging in measurements with long acquisition times *New J. Phys.* **14** 093027
[25] Kling N G *et al* 2013 Carrier-envelope phase control over pathway interference in strong-field dissociation of H_2^+ *Phys. Rev. Lett.* **111** 163004
[26] Li H *et al* 2015 Coherent electronic wave packet motion in C_{60} controlled by the waveform and polarization of few-cycle laser fields *Phys. Rev. Lett.* **114** 123004
[27] Kakehata M, Takada H, Kobayashi Y, Torizuka K, Fujihira Y, Homma T and Takahashi H 2001 Single-shot measurement of carrier-envelope phase changes by spectral interferometry *Opt. Lett.* **26** 1436–8
[28] Li C, Moon E, Wang H, Mashiko H, Nakamura C M, Tackett J and Chang Z 2007 Determining the phase-energy coupling coefficient in carrier-envelope phase measurements *Opt. Lett.* **32** 796–8
[29] Wang H, Chini M, Moon E, Mashiko H, Li C and Chang Z 2009 Coupling between energy and phase in hollow-core fiber based f-to-2f interferometers *Opt. Express* **17** 12082–9
[30] Koke S, Grebing C, Manschwetus B and Steinmeyer G 2008 Fast f-to-2f interferometer for a direct measurement of the carrier-envelope phase drift of ultrashort amplified laser pulses *Opt. Lett.* **33** 2545–7
[31] Lozovoy V V, Pastirk I and Dantus M 2004 Multiphoton intrapulse interferenc: IV. Ultrashort laser pulse spectral phase characterization and compensation *Opt. Lett.* **29** 775–7
[32] Nisoli M, Stagira S, Silvestri S D, Svelto O, Sartania S, Cheng Z, Lenzner M, Spielmann C and Krausz F 1997 A novel-high energy pulse compression system: generation of multigigawatt sub-5 fs pulses *Appl. Phys.* B **65** 189–96
[33] Sayler A M, Rathje T, Müller W, Kürbis C, Rühle K, Stibenz G and Paulus G G 2011 Real-time pulse length measurement of few-cycle laser pulses using above-threshold ionization *Opt. Express* **19** 4464–71
[34] Kling N G 2013 Controlling the dynamics of electrons and nuclei in ultrafast strong laser fields *PhD Thesis* Kansas State University
[35] Marceau C, Gingras G, Thomas S, Kassimi Y and Witzel B 2014 Energy-phase coupling inside sapphire-based f–2f nonlinear interferometers from 800 to 1940 nm *Appl. Opt.* **53** 898–901
[36] Lücking F, Trabattoni A, Anumula S, Sansone G, Calegari F, Nisoli M, Oksenhendler T and Tempea G 2014 *In situ* measurement of nonlinear carrier-envelope phase changes in hollow fiber compression *Opt. Lett.* **39** 2302–5
[37] Möller M, Sayler A M, Rathje T, Chini M, Chang Z and Paulus G G 2011 Precise, real-time, single-shot carrier-envelope phase measurement in the multi-cycle regime *Appl. Phys. Lett.* **99** 121108